National Defence / Défense nationale

# DESIGN AND DEMONSTRATION OF AN ACOUSTO-OPTIC TIME-INTEGRATING CORRELATOR WITH A LARGE A PARALLEL GAIN

by

N. Brousseau and J.W.A. Salt





DEFENCE RESEARCH ESTABLISHMENT OTTAWA
TECHNICAL NOTE 93-24



Canada

December 1993
Ottawa

National Defence / Défense nationale

# DESIGN AND DEMONSTRATION OF AN ACOUSTO-OPTIC TIME-INTEGRATING CORRELATOR WITH A LARGE A PARALLEL GAIN

by

**N. Brousseau and J.W.A. Salt**
*Electronic Support Measures Section*
*Electronic Warfare Division*



**DEFENCE RESEARCH ESTABLISHMENT OTTAWA**
TECHNICAL NOTE 93-24

PCN
041LQ

December 1993
Ottawa

## ABSTRACT

Time-Integrating Correlators (TICs) use either surface (integrated-optics) or bulk acousto-optic interactions. This technical note documents the development of a signal processor that includes a TIC designed to operate with a large parallel gain and a digital post-processor (DPP). The DPP controls both the input of signals to the TIC and the collection and analysis of optical data from the TIC. This note also reviews the principle of operation of TICs, discusses the selection criteria and compromises involved in selecting the various components, and describes the DPP, and presents the algorithms available to analyze the output of the TIC.



## RÉSUMÉ

Les effets acousto-optiques de surface (optique intégrée) ou de volume peuvent être utilisés pour la mise en oeuvre de Corrélateurs à Intégration Temporelle (CIT). Le but de cette note technique est de décrire le développement d'un système de traitement des signaux qui inclut un CIT à gain parallèle élevé et une Unité de Post-Traitement Numérique (UPTN). L'UPTN contrôle les signaux d'entrée du CIT ainsi que la collecte et l'analyse des données optiques produites par le CIT. Une brève revue des principes d'opération d'un CIT ainsi qu'une discussion des critères de sélection des diverses composantes et des compromis nécessaires sont présentés. L'UPTN et les algorithmes d'analyse des données de sortie du CIT sont aussi décrits.

## EXECUTIVE SUMMARY

Time-Integrating Correlators (TIC) are particularly suitable for processing long duration, large bandwidth, data strings. However, their most important feature is their capability to perform correlation, in parallel, over a wide range of relative time-delays. This feature provides a large parallel gain and makes signal acquisition easier. High-quality laser light sources, photodetector arrays, and Bragg cells make it possible to produce high-performance optical data processors.

The TIC presented in this technical note is an acousto-optic data processor that produces a cross-correlation between any two RF input signals without requiring time-inversion of one of the signals. It is designed to operate with a large parallel gain and a digital post-processor (DPP). This note reviews the principle of operation of TICs and, discusses the criteria and compromises involved in selecting the various components. The compromises involved in the selection of an Helium-Neon laser, of tellurium dioxide Bragg cells and of the techniques used to expand the laser beam are discussed. The imagining system, constructed from commercially available lenses, and the detector array are described.

The DPP controls both the input of signals to the TIC and the collection and analysis of optical data from the TIC. This note also presents the algorithms used to analyze the output of the TIC. The algorithms developed for pedestal removal and for statistical analysis of results produced by the TIC are described.

## TABLE OF CONTENTS

## LIST OF FIGURES

LIST OF FIGURES (cont'd)

## LIST OF TABLES

## LIST OF ABBREVIATIONS

| | |
|---|---|
| CCD | Charge-coupled device |
| CRC | Communications Research Centre |
| DNA | Deoxyribose nucleicacid |
| DPP: | Digital Post-Processor |
| DREO | Defence Research Establishment Ottawa |
| RF: | Radio Frequency |
| $TeO_2$: | tellurium dioxide |
| TIC: | Time-Integrating Correlator |
| USAF | United States Air Force |

## 1.0 INTRODUCTION

High-quality sources of laser light, photodetector arrays and Bragg cells make it possible to produce high-performance optical data processors. The time-integrating correlator (TIC) presented in this technical note is an acousto-optic data processor that produces a cross-correlation between any two radio frequency (RF) input signals whose down-converted versions are within the bandwidth of the Bragg cell.

TICs are particularly suitable for the processing of long duration, large bandwidth, data streams (for example, the streams used in spread-spectrum communications). The correlation signal produced by a TIC contains information about the parameters of the signal that is being processed. A correlation peak indicates that two nearly identical data streams have been received. The shape and location of this peak contain information that can be used to determine the carrier frequency, the modulation rate, and the difference in time of arrival of the signals. However, the most important feature of TICs is their capability to perform correlation, in parallel, over a wide range of relative time-delays. This feature provides a large parallel gain, and makes signal acquisition easier. Applications such as spread-spectrum processing [1-3], fine-delay estimation of time of arrival [4], passive surveillance [5, 6], and analysis of deoxyribose nucleic acid (DNA) [7] have been proposed for TICs.

TICs use either integrated-optics [1-3,5-6,8-13] or bulk [4,7,14-25] acousto-optic interactions. This technical note documents the development of a signal processor that includes a TIC designed to operate with a large parallel gain and a digital post-processor (DPP). The DPP controls both the input of signals to the TIC and the collection and analysis of optical data from the TIC. The principle of operation of TICs and the criteria and compromises involved in selecting various components are discussed in Sections 2.0 and 3.0. The DPP which controls the flow of data to and from the TIC, and the algorithms developed to analyze the output of the TIC are described in Section 4.0.

## 2.0 DESCRIPTION OF A TIME-INTEGRATING CORRELATOR

TICs based on amplitude modulation of laser beams use either integrated-optics [1-3,5-6,9,12] or bulk [7,15-19] acousto-optic interactions. In acousto-optic systems, a modified Mach-Zehnder configuration is used. Thorough theoretical analyses of these systems are available [1,12,17,24]: therefore, only those aspects related to the design of a system with a large parallel gain are reviewed.

In the system shown in Figures 1 and 2, the beam produced by the HeNe laser is expanded and then divided into two equal intensity paths by a cube beam-splitter. The two beams are then redirected (at the Bragg angle) onto the Bragg cells, by two folding mirrors (M1 and M2). A photograph of the system is presented in Figure 2. The two RF inputs that carry digital modulation are applied to the Bragg cells to amplitude-modulate

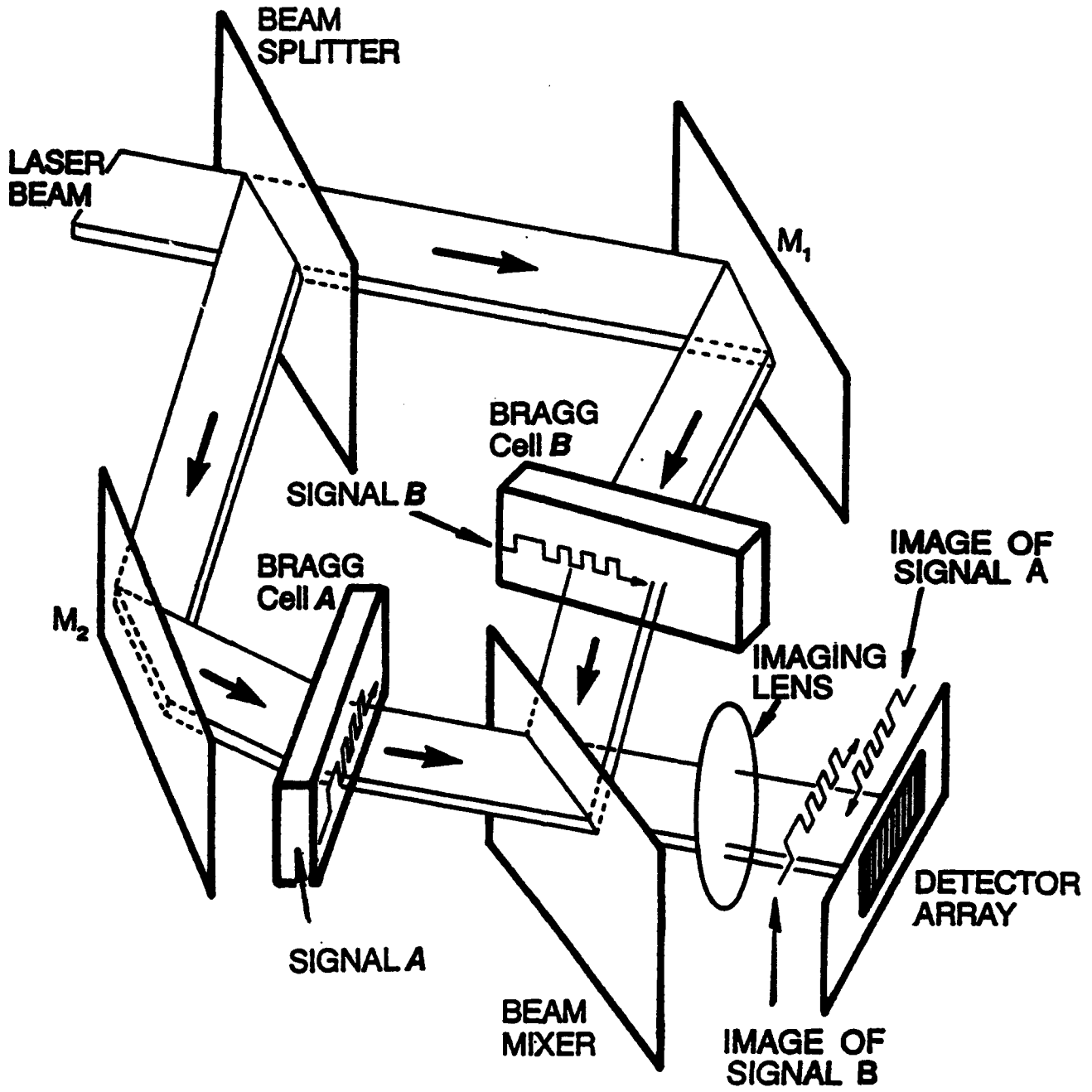


Figure 1: Schematic Diagram of a Mach-Zehnder Time-Integrating Correlator

a)

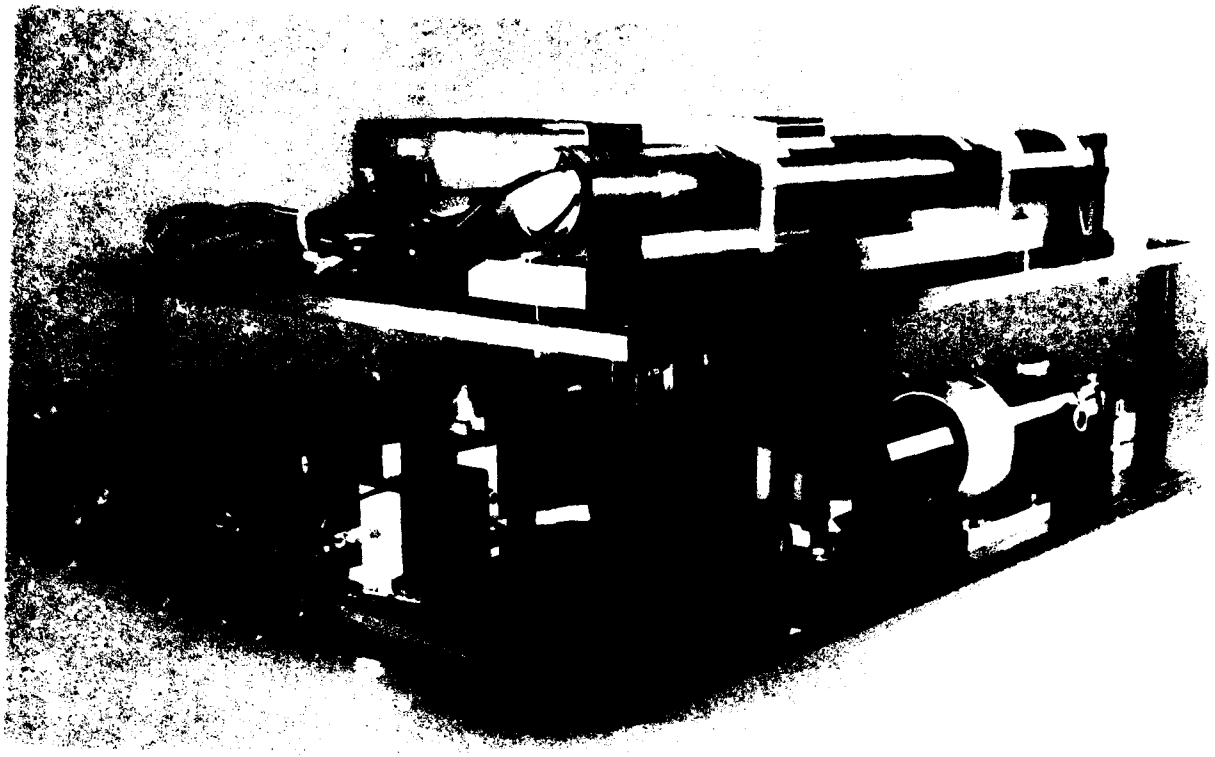

b)

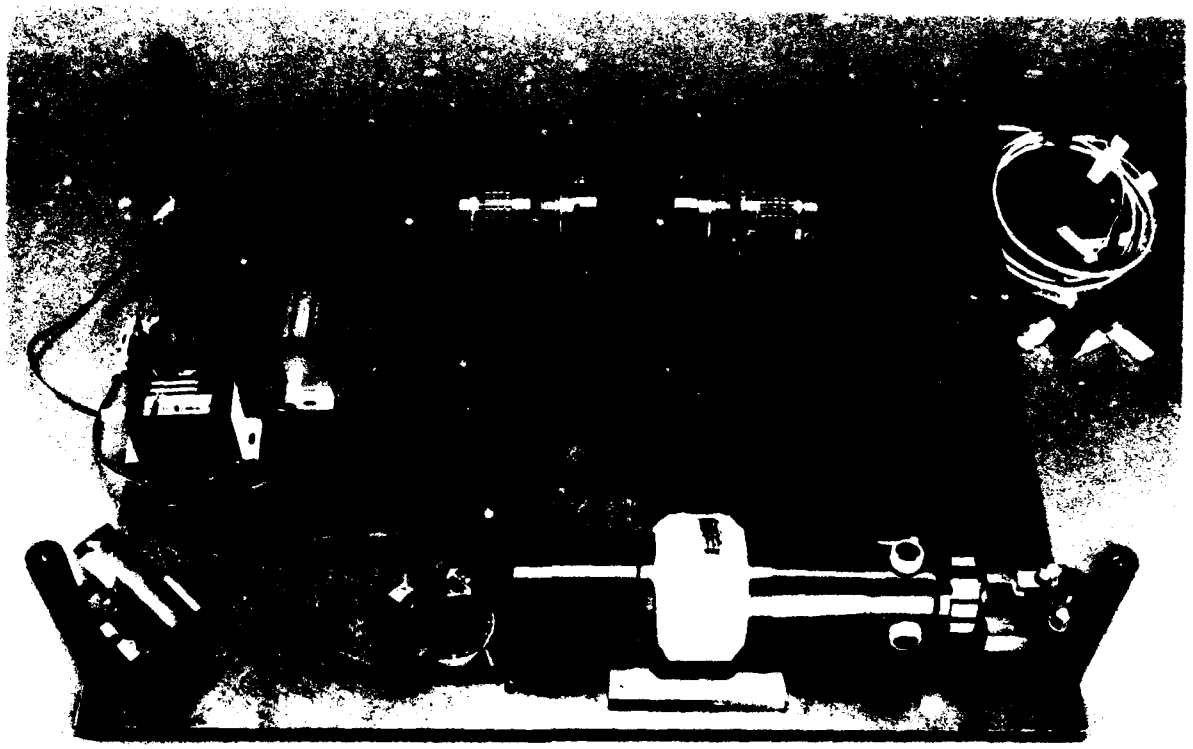

Figure 2: Photograph of the Mach-Zehnder Time-Integrating Correlator Developed at DREO
a) the whole system with the laser and its power supply on the top level,
b) the interferometer.

the expanded laser beams through a bulk acousto-optic interaction. Because no bias is used in the linear modulation process, a maximum dynamic range is produced. The two diffracted light distributions carry the information contained in the two RF signals that were applied to the Bragg cells. The diffracted light beams are mixed and imaged on the detector array to be counterpropagating. The elements of the detector array perform coherent addition and time-integration of the two signals. The signal S(T,z) produced by the detector array can be described as:

$$S(T,z) = \int_T |A(t+z/v) + B(t-z/v)|^2 \, dt \qquad (1)$$

$$s(T,z) = \int_T A^2(t+z/v)\,dt + \int_T B^2(t-z/v)\,dt + 2\int_T A(t+z/v)\,B^*(t-z/v)\,dt \qquad (2)$$

where A(t) and B(t) are the signals applied to the Bragg cells, t is the time, T is the integration time of the detector array, v is the velocity of the acoustic signal in the Bragg cells, and z is the distance along the Bragg cells (z=0 is located at the centre of the Bragg cells). The * represents the complex conjugate. The t+z/v and t-z/v terms represents the fact that the signals propagated in the Bragg cells are imaged to be counterpropagating on the detector array. This counter-propagation, combined with the time-integration performed by the detector, is essential to the production of a correlation.

The typical output of a TIC that is performing an auto-correlation is characterized by a peak that appears over a pedestal. The $A^2$ and $B^2$ terms in equation [2] contribute to the formation of the pedestal (see Figure 3). The correlation peak is produced by the AxB term, at the meeting point of the two counterpropagating signals on the detector array. The correlation peak can be observed over a range of time delays that is equal to twice the time $\tau$ it takes the signal to propagate through the Bragg cells. To facilitate the detection of the peak, the pedestal is removed. The presence of the correlation peak can be confirmed by using a threshold signal.

In TIC that was developed by DREO, the light beams are amplitude modulated by the acoustic waves, rather than intensity (power) modulated. Linear-amplitude modulation is possible when the diffraction efficiency of the Bragg cell is low, and because no bias is used, a better dynamic range is available for signal processing [12 (p.291), 25].

a)

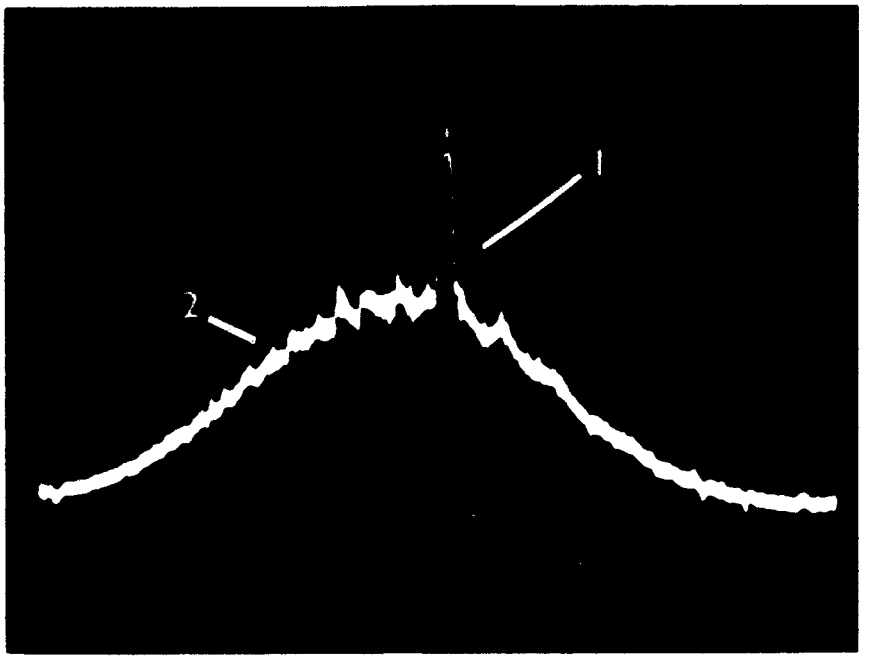


b)

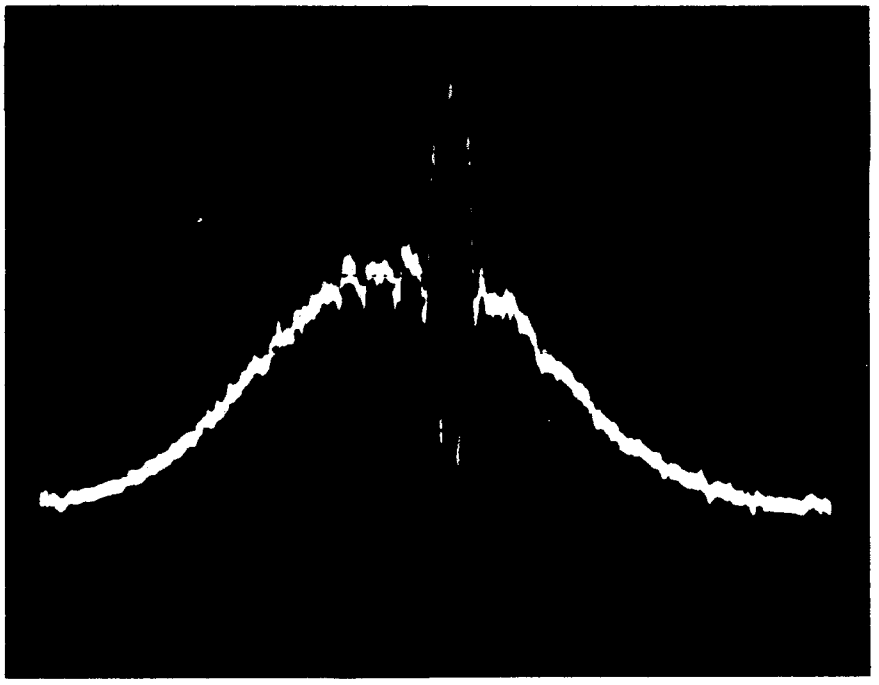

Figure 3: A Correlation peak on a pedestal.
a) without fringes 1) peak;
2) pedestal,
b) with fringes.

The parallel processing gain ($G_p$) is determined by the number of bits present in the Bragg cells. The gain is equal to the product of the bit rate (B) of the signal and the time-delay window $2\tau$ of the TIC.

$$G_p = 2\tau B \tag{3}$$

## 3.0 SELECTION OF THE COMPONENTS OF A TIME-INTEGRATING CORRELATOR

The selection of components for a TIC with a large parallel gain involves many compromises. Limitations are imposed by the availability of components and by constraints on the size and complexity of the final system. More than one good solution is available. However, the set of choices presented in this technical note was found to be most appropriate given the constraints that were faced.

### 3.1 Bragg Cells

The key components of a TIC with a large parallel gain are Bragg cells with a large time-aperture $\tau$. The length of the Bragg cells must be kept to a manageable dimension. Therefore, in optical materials with a slow acoustic velocity of propagation (v) and with a low attenuation of the acoustic waves are used to obtain a large time-aperture. Large time-aperture devices are usually made of tellurium dioxide ($TeO_2$) operating in the slow-shear mode. Devices with time-apertures as large as 100 $\mu$s are available commercially. The dynamic range, polarization, and frequency response of Bragg cells have been extensively studied and are well documented [26-30]. Because the velocity of acoustic waves in $TeO_2$ is 620 m/s, a device with a 100-$\mu$s aperture device is 62-mm long. To take advantage of the full interaction time of these Bragg cells, the whole aperture must be illuminated. The signals propagating in the Bragg cells must also be imaged on the detector array. These operations are not easy with a 62-mm aperture. A compromise between maximum parallel gain and implementation difficulties was reached by building the first system with Bragg cells that had a time-aperture of 50 $\mu$s (31-mm aperture).

It is also desirable that the TIC produce correlation peaks that are of uniform amplitude over the aperture of the Bragg cells. This requires that the exponential attenuation in the Bragg cells be compensated for by selecting the appropriate part of the Gaussian distribution of the illumination beam for each Bragg cell. The distribution of diffracted light is flattened if only 40 $\mu$s of the 50 $\mu$s aperture of the Bragg cells is used. Narrowing or tapering the illumination profile also helps control the parameters of the Gaussian distribution of the illuminating beam. A TIC with a time-aperture of 40 $\mu$s time-aperture of 40 $\mu$s that is operated at 20 MHz has a parallel gain of 1600.

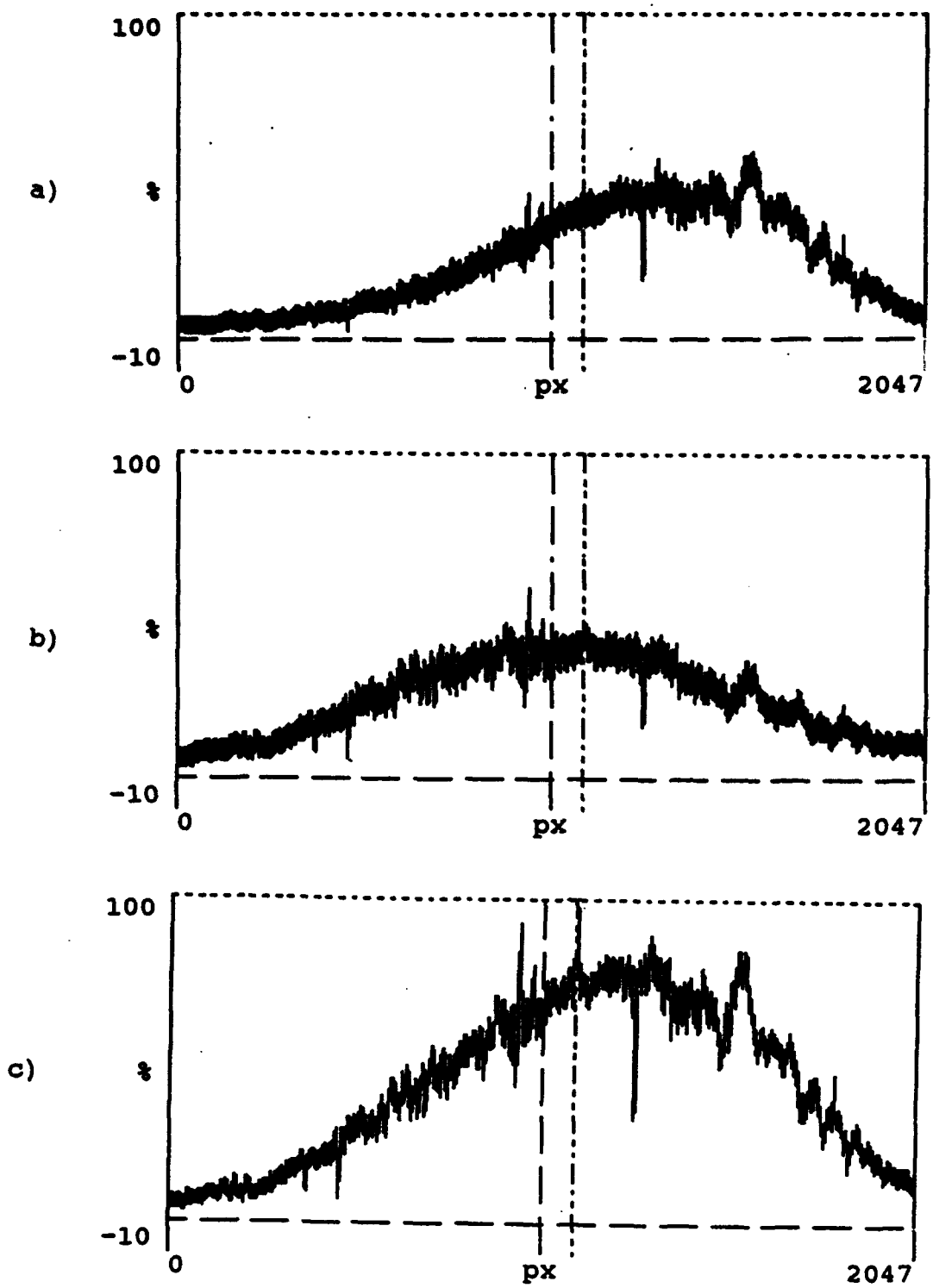


**Figure 4:** Light diffracted by the Bragg cells
a) from Bragg cell A,
b) from Bragg cell B, and
c) from the two Bragg cells.

Figure 4 illustrates the intensity distributions produced for one particular adjustment of the TIC. Part A is the light diffracted by Bragg cell A, Part B is the light diffracted from Bragg cell B, and Part C is the combined output from both Bragg cells.

### 3.2 Beam Expansion

A large time-aperture TIC requires large mirrors and beam-splitters, which tend to become heavier and more expensive as they increase in size. Expansion of the laser beam is also a problem because pinhole spatial filtering is necessary to remove the noise generated by non-uniformity of the laser beam (see Figure 5, a and b). Beam expanders with pinhole filtering and a 100-mm diameter aperture are available commercially, but they are large and heavy. Similar 50-mm diameter beam expanders are more manageable, but they require other techniques (for example, prisms [31-33]) to increase their effective diameter to 62 mm. However, the use in the prototype of a 25-mm long section of Bragg cells with a time-aperture of 40 $\mu$s reduced complexity and enabled the use of a 50-mm beam-expander without a prism.

The light budget is also important. When a 100-mm diameter beam expander is used, less than 1% of the energy falls on the centred 1 x 62-mm aperture of the Bragg cells. When a 50-mm beam expander is used to illuminate the 1 x 25-mm Bragg cell apertures, 2% of the available energy is provided to the Bragg cells and greater flexibility is available to select an appropriate section of the Gaussian profile. Therefore, smaller Bragg cells combined with a smaller beam expander seem preferable.

The diffraction efficiency of Bragg cells decreases exponentially as the distance from the transducer increases. The transducer uses the piezoelectric effect to transform, the RF signal applied to the Bragg cells into a travelling modulation of the index of refraction of the crystal. What really matters is that the product of the illumination pattern with the attenuation function of the Bragg cells be as uniform as possible. Figure 4 shows typical light distributions that were generated when the best 25-cm segment of the Bragg cell was illuminated with a selected 25-mm segment of a 50-mm beam expander.

The quality of the wavefront produced by the beam expander was evaluated using a beam-shearing interferometer. The interferogram illustrated in Figure 5c shows that a small amount of aberration causes the fringes to curve slightly. The fringes associated with a perfectly flat wavefront would be straight. The wavefront error in this interferogram is $\lambda/4$.

a)

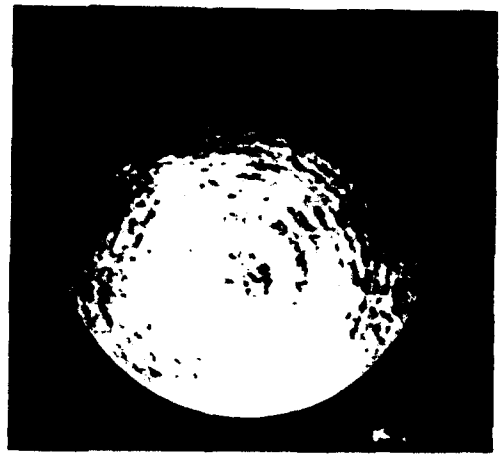

b)

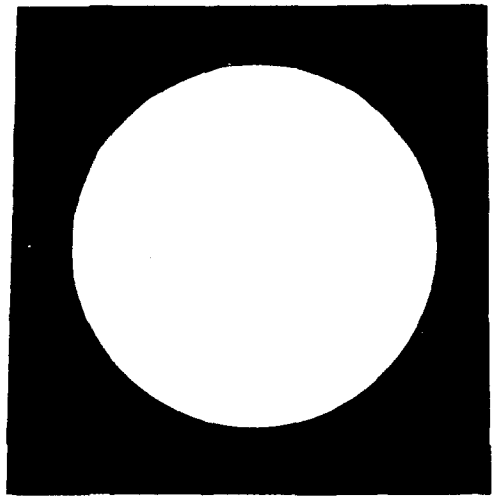

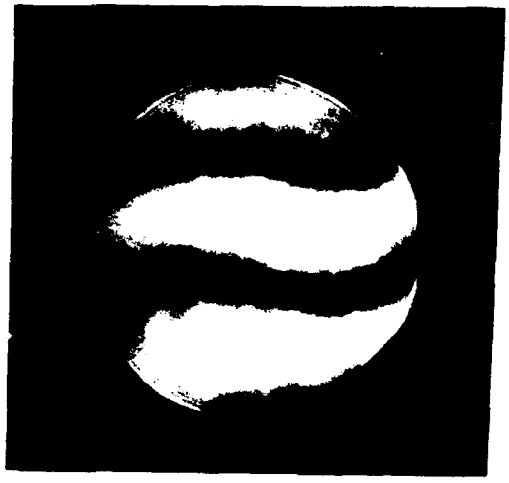

**Figure 5:** Output of the Beam-Expander
a) without pinhole filtering,
b) with pinhole filtering, and
c) beam-sharing interferogram of the illumination beam.

### 3.3 Beam-Splitters, Beam-Mixers, and Mirrors

The design of a TIC that uses the Mach-Zehnder interferometric layout (Figures 1 and 2) has minimum degrees of freedom. It relies on accurate machine shop practice to mount the components precisely. The mirrors M1 and M2 in the interferometer rotate about their vertical axis and can be adjusted using a knob and lockable set screw. The folding mirrors are mounted on a rotation stage as are the beam splitter and the beam mixer. Cube beam-splitters and mixers with 50-mm aperture and a flatness of $\lambda/20$ are needed to illuminate the 25-mm effective aperture of the Bragg cells.

### 3.4 Imaging System

The imaging system was made using two Pentax SMC 85 mm camera lenses set back-to-back. The two lenses operate at close to optimal conditions: because parallel light enters the first lens and is focused in the Fourier plane. The light then diverges and is transformed again into a parallel beam by the second lens. This compact symmetrical configuration that can be adjusted to produce images with a magnification close or equal to one. Because the Fourier plane is easily accessible it can be used to perform bandpass filtering, remove the undiffracted light, or possibly, undertake interference excision [12 (p.127),30].

The quality of the wavefront of the output beam was checked using a beam-shearing interferometer. Figure 6 shows the interferograms that were produced when the focus of the lenses was set at $\infty$ and 0.85 m with focal lengths of 85 mm and 77 mm, respectively. The beam-shearing interferogram of the incident illuminating beam is shown in Figure 5c. The effects of spherical aberration [34] are visible. As expected, better results were obtained when the focus of the lenses was set at $\infty$. The quality of the wavefront produced when the focus was set at $\infty$ is certainly sufficient to demonstrate the success of the prototype. The resolution of the imaging system was measured using a high-contrast USAF test target, and it was found to be at least 200 lines/mm over the central 25-mm section of the image field for at magnification of one.

### 3.5 Laser Selection

A few important factors must be taken into account when selecting the source of laser light for a TIC. Some of these requirements are conflicting; therefore, compromises must be made. For example, a very small laser is easier to package. However, the laser must produce enough power to operate the system, and small lasers produce small power output. Another selection criterion is the stability of the mode of output of the laser. The laser must be operated in the fundamental mode, which is characterized by a Gaussian distribtuion of the output light.

a)

b)

**Figure 6:** Beam-shearing interferograms of the wavefront produced by the imaging system
a) focus at ∞ and focal length 85 mm,
b) focus at 0.85 m and focal length 77 mm.

Other transversal modes, which produce light distributions having bright and dark spots are unacceptable. The amount of heat dissipated by the laser is also a concern because it affects the thermal stability of the whole TIC.

The laser must also operate at a wavelength for which a sensitive linear detector array is available to detect the light distributions produced by the TIC. This limits the range of wavelengths to the visible and near infrared. The red end of the spectra is preferred because the PIN photodiodes that are used as detectors are most sensitive to red light. Reliability is also important.

The two obvious choices were HeNe lasers and laser diodes. Laser diodes operating at 850 nm were seriously considered, but they were rejected because of their cost and the unacceptable delays that were associated with conversion from HeNe visible light to laser diode near-infrared invisible light. The cost and delays were caused mainly by the replacement of the optical components that had anti-reflection costing for HeNe with components that had anti-reflection coating for laser diodes at 850 nm, and by the procurement of new Bragg cells that were optimized to operate at that laser wavelength. A 10-mW HeNe laser was selected because of its well-established record for reliable, trouble-free operation. As well, all of the optical equipment has an anti-reflection coating for that wavelength.

When this work was done, visible laser diodes operating at about 630 nm with sufficient power and stability were under development, but they were not yet available. These diodes should be considered when their performance has been improved.

### 3.6 Detector Array

A Thompson CSF TH 7805 detector array was used to supply data to the DDP in the first prototype of the Mach-Zehnder TIC. This detector array has 2048 elements that are each 13 $\mu$m X 13 $\mu$m in size. The signals from the odd and even number elements are clocked by two different CCD shift registers at a maximum rate of 10 MHz; therefore, the overall equivalent read-out rate is 20 MHz. This feature limits the minimum integration time to 104 $\mu$s. The longest integration time possible with the present system is 416 $\mu$s, which is limited by the DDP. The dynamic range of the detector array was measured to be 22 db [35]. Other detector arrays have been acquired and will be tested. A better detector array will be included in a more advanced version of the TIC.

### 3.7 Packaging

The original package was designed to allow the TIC to be installed in a 19 inch (48-cm) rack, and to explore the requirements for stable operation. The frame, component supports, and layout were designed by DREO staff and manufactured in the CRC machine shop. This work was based on the design and

demonstration of the first "breadboard". Special care was taken to minimize the degrees of freedom for the alignment of the components. A combination of commercial and custom-designed holders was used to make the system as rigid as possible. The laser and its power supply were installed above the rest of the optics (see Figure 2a). This design facilitates the dissipation of the large amount of heat generated by these two components. The laser beam is taken down to the lower level by a system of two penta-prisms and this enables the system to fit a 19-inch rack more easily.

Although the optical stability was far better after packaging, it was still unsatisfactory because of the nature of the Mach-Zehnder layout, which has numerous components and widely separated optical paths. These paths may suffer independent effects from vibrations and thermal disturbances that can reduce their stability. Therefore, it was decided to explore other architectures that would require less components, be more compact, and would consequently be easier to package and more likely to provide stable performance. It was also decided that, if possible, the final packaging of the operational system should be done by a specialized firm.

## 4.0 THE DIGITAL POST-PROCESSOR

Most operations of the TIC are controlled by the DPP. The DPP (Figure 7) controls the flow of signals to and from the TIC and the associated hardware and software. The DPP provides the operator interface [36] and allows parameters of operation (for example, the integration time, the type of display for the results, and the type of pedestal removal) to be defined. The DPP also contains the algorithms used for statistical analysis of the results from the TIC. Most of the results in this technical note were collected using the TIC and its DPP.

The DPP is designed to be a research tool; therefore, it has a large amount of flexibility. This flexibility is achieved by the use of software rather than hardware [37-38] to implement the processing algorithms. Although this leads to slow operation, it is acceptable for a prototype whose main purpose is to test the processing algorithms. However, hardware will be used to implement most of the algorithms that will be included in future upgrades of the system.

### 4.1 System Configuration

The system runs in the Microsoft Windows (2.11) operating environment under the MS-DOS 2.04 operating system on an 286 IBM AT-compatible computer [36]. Windows provides a graphics interface under which several tasks can run concurrently. Standard mouse, keyboard, screen and printer interfaces are provided. The post-processor consists of several independent

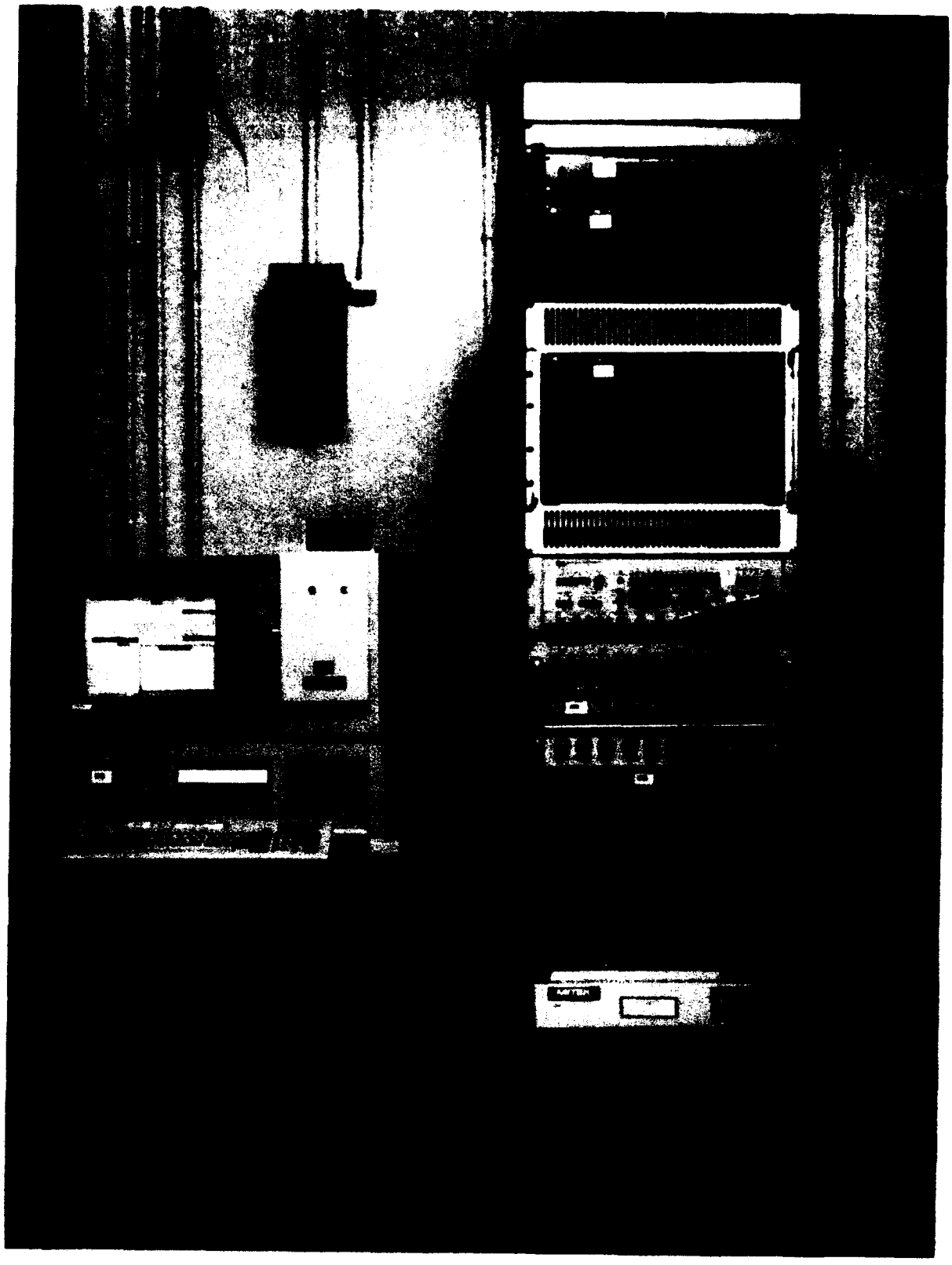

**Figure 7: Photograph of the Digital Post-Processor (DPP)**

tasks that run concurrently and communicate using the Dynamic Data Exchange protocol and a few special messages. The system is implemented in the C computer language, and includes some Assembler routines where necessary. The Microsoft C 5.1 compiler and Microsoft Macro Assembler 5.1 were used. An IEEE-488 Controller is the serial interface between the computer and the other components of the system. Table 1 lists the main pieces of equipment in the DPP.

TABLE 1: LIST OF EQUIPMENT USED TO IMPLEMENT THE SPREAD-SPECTRUM PROCESSING FACILITY

| |
|---|
| 80286 computer (8 MHz)<br>640 Kb RAM, 1 Mb expanded memory<br>AT style keyboard<br>EGA adapter<br>80287 coprocessor<br>2 removable hard disks<br>360 Kb 5 1/4-inch floppy disk drive<br>1.2 Mb 5 1/4-inch floppy disk drive<br>mouse |
| High-Resolution colour graphics monitor |
| IOtech Micro488 RS-232C to IEEE-488 bus controller |
| Laser printer |
| AYDIN Pattern Generator Model 2712G |

The DPP hardware processes [39] the output from the TIC without intervention from the host processor. This includes pedestal removal (see Section 4.2), and the detection of correlation peaks above a specified threshold. The detection of a correlation peak is declared as soon as the threshold has been met M times. N trials are allowed. It is also possible to add many TIC outputs, each of them collected with an integration time (T), to increase the effective integration time. Hardware is available to perform phase-shift pedestal removal for the carrier frequencies and bandwidths that correspond to the various types of TICs that were studied at DREO (see Table 2). Processing within the correlator is performed in real time at pixel rates that are the same as the read-out rate of the pixels in the detector array (10 MHz). It was decided to test the system using direct sequence spread spectrum signals employing maximal-length sequences (m-sequences) [40] as spreading codes. The m-sequences are designated by an octal number representing their generating

polynomial. We use the notation described in [40]. These signals are wideband signals which produce a nearly ideal single triangular correlation peak of known width. Correlation of these signals represents the applications of detecting a known signal in noise, or of determining the direction of arrival of a direct sequence signal by correlating the signals received from two spaced antennas.

The host processor programs the hardware when a new sequence of bits is sent to the TIC from the AYDIN pattern generator. Multiple sequences are stored in a file and processed in a sweep through the file.

TABLE 2: CHARACTERISTICS OF THE PHASE-SHIFT MODULES INCLUDED IN THE DIGITAL POST-PROCESSOR HARDWARE

| Characteristics of Bragg Cell | Bandwidth | Center Frequency |
|---|---|---|
| glass (bulk interaction) | 100 MHz | 150 MHz |
| $LiNbO_3$ (integrated optic interaction) | 80 MHz | 400 MHz |
| $TEO_2$ (bulk interaction) | 30 MHz | 45 MHz |
| $TEO_2$ (bulk interaction) | 50 MHz | 75 MHz |

When a correlation peak is detected, information (for example, location, amplitude, and width) is extracted and presented to the operator. The fringe-period determination and power-spectrum computation can also be performed. The analysis of a correlation function in the host processor is not performed in real time.

The three states of operation [38,39] of the TIC are Idle, Run, and Calibrate (see Figure 8). In the Idle state, the parameters of the correlator and code generator can be changed. As well, control options can be changed, and the other states can be entered. In the Run state, the correlator is programmed to search for correlations between the input signal and one or more codes. Detected correlation peaks are analyzed and the results are presented either on the screen or the printer. Results may also be saved on disk. The Run state terminates when the programmed operations are completed, when a detection occurs, or when the operator halts the program. At termination, the system returns to the Idle state.

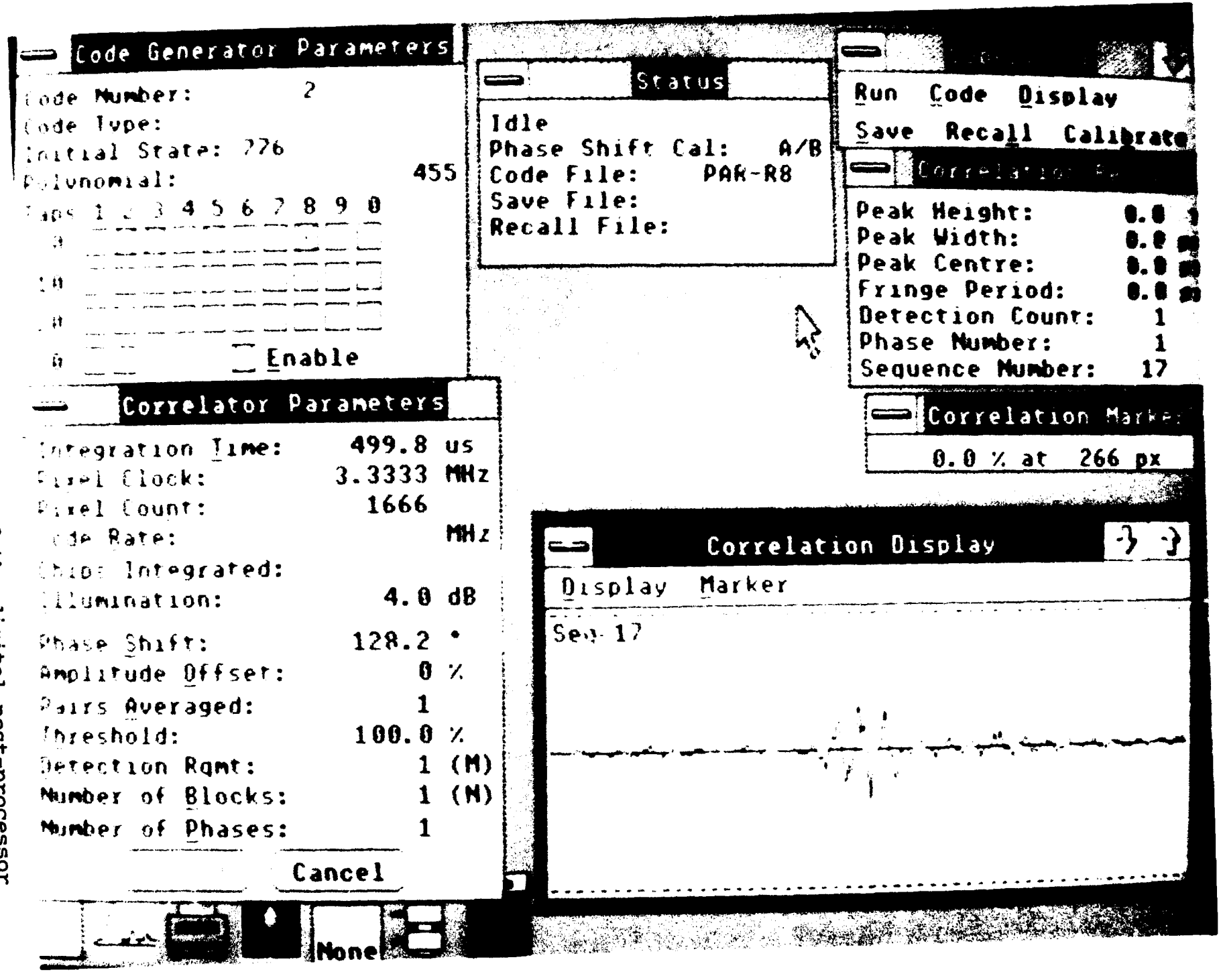


Figure 8: Some of the windows of the digital post-processor.

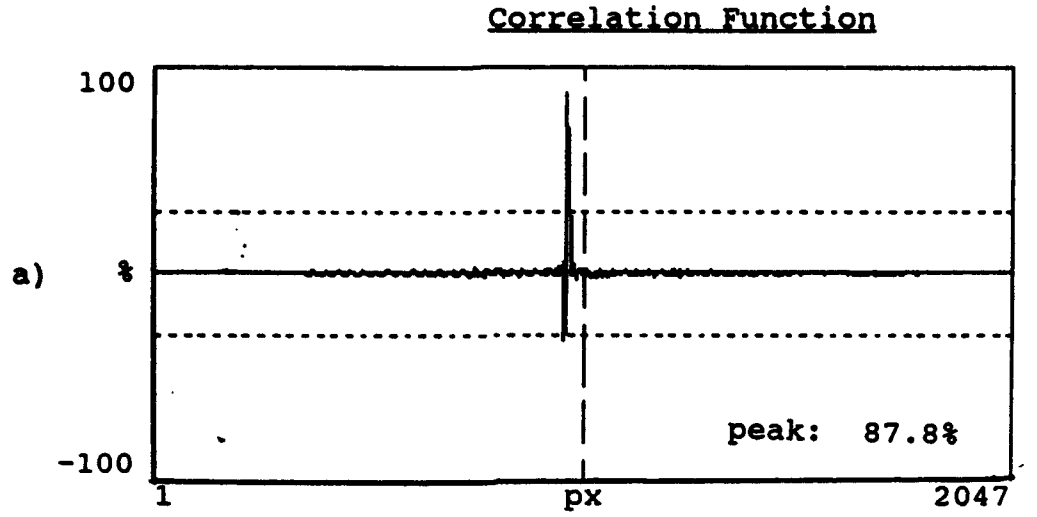


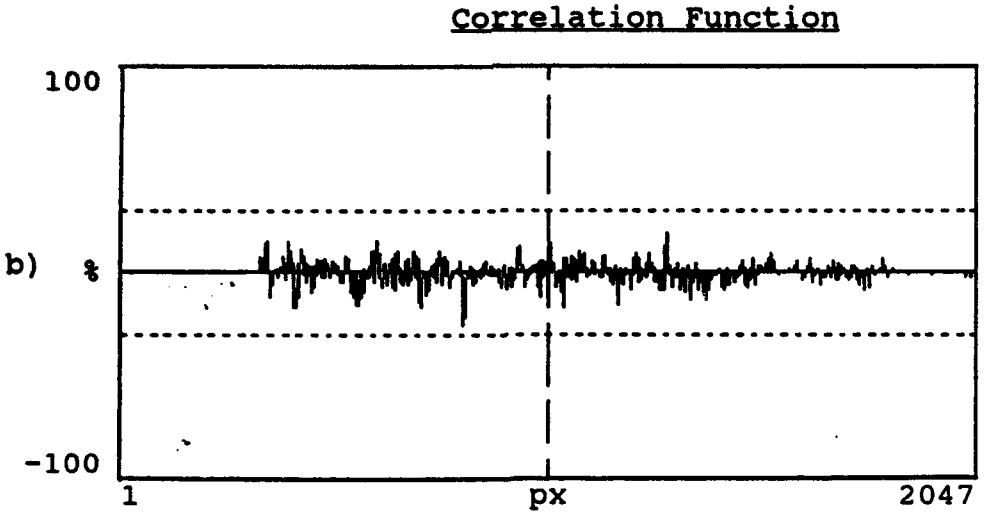


Figure 9: Example of pedestal removal with the phase-shift removal technique.
a) autocorrelation of m-sequence 717,
b) cross correlation of m-sequence 615 by 717 where the m-sequence are designated by an octal number representing their generating polynomial according to the notation described in [40].

Three types of calibration can be performed in the Calibrate state. In phase calibration, the system calculates the phase shift required to maximize the cross-correlation function of the two RF inputs. In amplitude calibration, the system calculates the amplitude offset required to optimize pedestal cancellation. In sensitivity calibration, the correlator is programmed to generate the characteristics of correlation sensitivity. When the calibration operations are complete, or when the operator halts them, the Calibrate state terminates, and the TIC returns to the Idle state.

## 4.2 Algorithms for Pedestal Removal

The DPP includes three algorithms for pedestal removal (see Section 2.0). In all three techniques, data collected during the previous integrations are subtracted from the current data to remove the pedestal. The first method [1,12] consists of subtracting two successive frames. The second frame is collected when a 180° phase shift of the RF signal is applied to one of the Bragg cells. This technique removes the pedestal and produces a positive peak whose amplitude (see Figure 9) is twice the amplitude of the peak of the frames used for the subtraction.

Figure 9 illustrates autocorrelation and cross correlation of a maximum-length pseudorandom direct sequence that was produced by the AYDIN pattern generator. Because of one of the fundamental properties of maximum length direct sequences [41], the autocorrelation exhibits only one high-amplitude peak (Figure 9a); whereas, the cross correlation contains many minor peaks (Figure 9b). This fact has an impact on the threshold for peak detection. The DPP includes the hardware and software needed to perform phase-shift pedestal subtractions for the four different combinations of bandwidth and centre frequency that are associated with the different types of Bragg cells (see Table 1).

The second technique for pedestal removal (see Figure 10) subtracts previously acquired pedestal that is refreshed at a rate defined by the user. This method requires a technique of data collection that always produces positive peaks.

In the third method (see Figure 11), the last frame that is collected (if it does not contain a peak) contributes a percentage to the pedestal level used for the subtraction. The pedestal values are updated after each frame is collected and the current pedestal is used to remove the pedestal from the frame just collected.

The second and third methods produce peaks (see Figures 10a and 11a) with half the amplitude of the peaks produced by the phase-shift method (see Figure 9a). However, the signal-to-noise ratios of the three methods should be the same. This can be verified, to a good approximation, by comparing the results of Figures 9, 10 and 11.

## 4.3 Packages for Statistical Analysis

Three different programs have been included in the DPP for statistical analysis. The first program [42] allows the operator to request the calculation of the mean, the variance, and the standard deviation of the amplitude of a segment of a correlogram specified by the operator. The parameters of the statistical analysis are set by the user. The statistical analysis window and an example of the results are presented in Figure 12. The user can request an analysis of two different segments of the correlogram. Each range must be defined by its first and last pixel. The program is executed by activating the analyze button, and the results are displayed on the screen when the calculations are finished. For each of the two segments, the number of pixels in each segment, the maximum amplitude found in the selected ranges, the location of the maximum amplitude, the average amplitude, and the variance and the standard deviation of the amplitude distribution are presented. These results can be printed (see Figure 12b).

With the second program [42], repetitive tests can be defined and statistics on the detection of a correlation peak and on the position and height of the peak can be calculated. Probabilities of detection and of false alarms can also be calculated. The detection statistics window and the resulting statistical report are illustrated in Figure 13.

The third program [43] is used to calculate probability distributions. Figure 14 shows the windows that control the calculation of the probability distribution of the correlograms and display of the results. Printed results are illustrated in Figure 15. The package allows the user to specify up to ten points on the correlograms on which to calculated probability distributions.

The operator must specify whether each location is on a peak or in the noise. At most, seven noise or seven peak values can be selected at one time. A histogram of the absolute value of the amplitude for each specified pixel is accumulated. The window illustrated in Figure 14a allows the user to select the type of results that will be calculated from the histogram. These results are displayed in the format illustrated in Figure 14b. It is possible to calculate and display the probability-density function or the cumulative-distribution function for the currently selected pixel. In addition, when the cumulative-distribution function is displayed, it can be overlaid with the corresponding Gaussian distribution. A pixel report (see Figure 15) or a P (tail) report (see Figure 16) can be selected from the print menu. The pixel report reproduces the information that is currently displayed in the statistics window. The P (tail) report displays and prints information about the tail probabilities of the histograms for every pixel selected in the

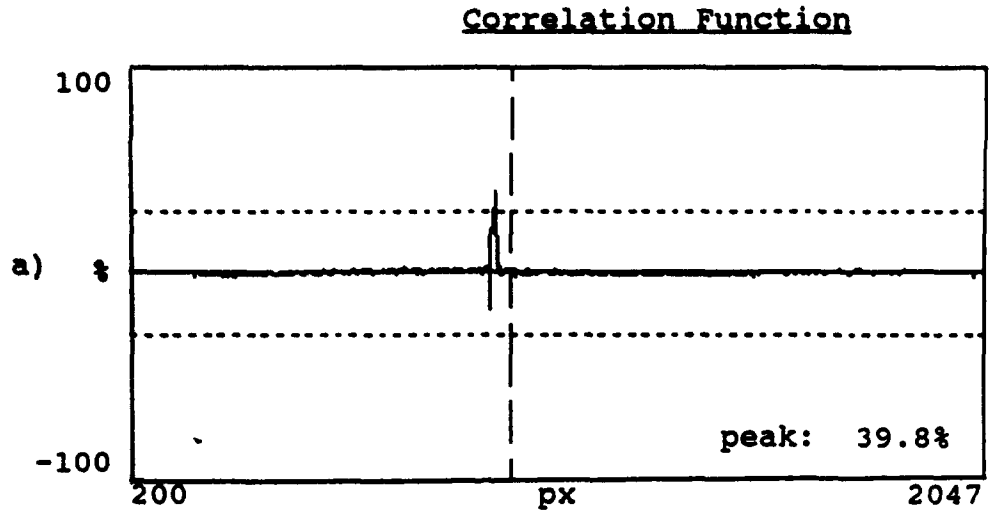


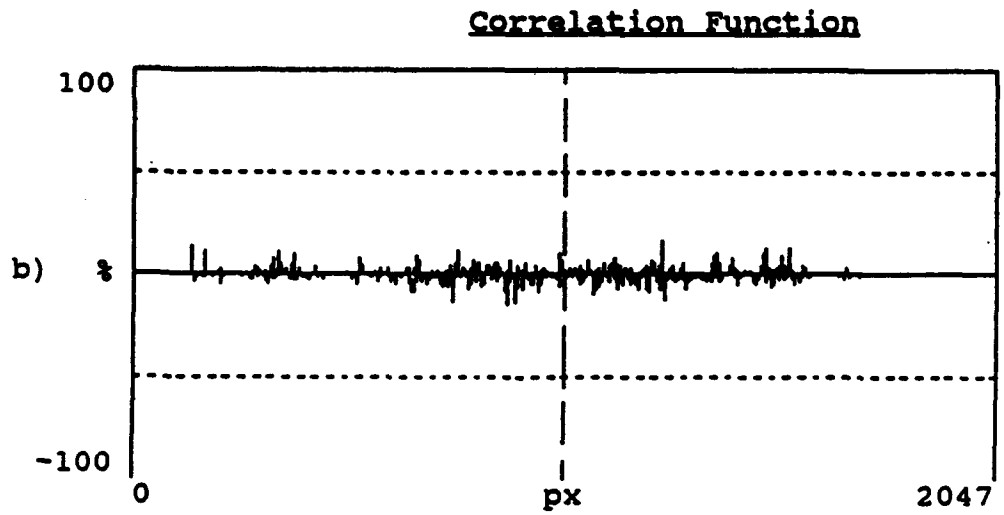


Figure 10: Example of pedestal removal with the refreshed pedestal technique.
a) autocorrelation of m-sequence 717,
b) cross correlation of m-sequence 615 by 717 where the m-sequence are designated by an octal number representing their generating polynomial according to the notation described in [40].

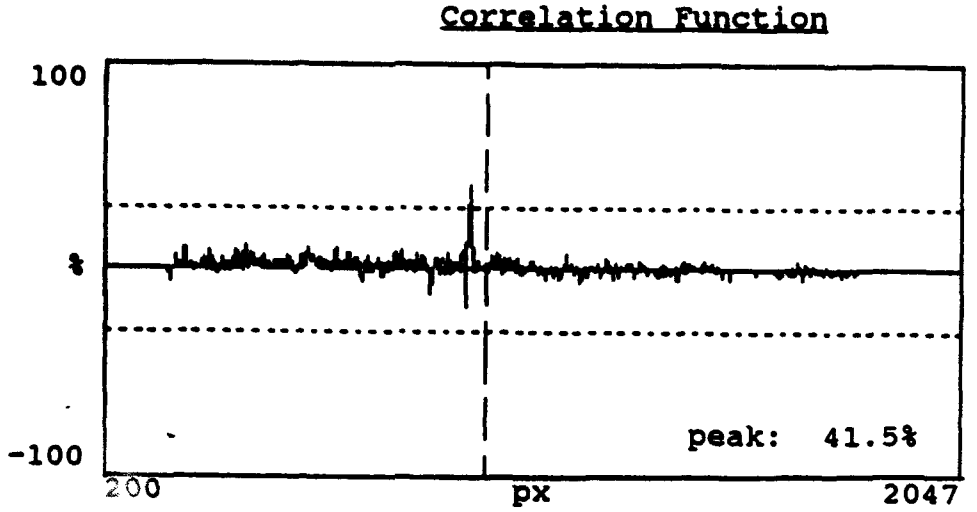


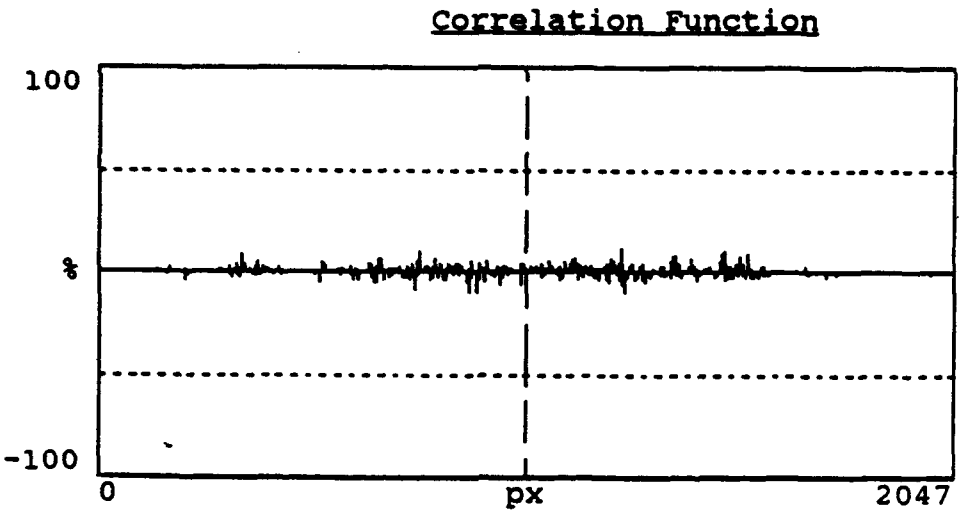


**Figure 11:** Example of pedestal removal with the averaging technique.
a) autocorrelation of m-sequence 717,
b) cross correlation of m-sequence 615 by 717 where the m-sequence are designated by an octal number representing their generating polynomial according to the notation described in [40].

a)

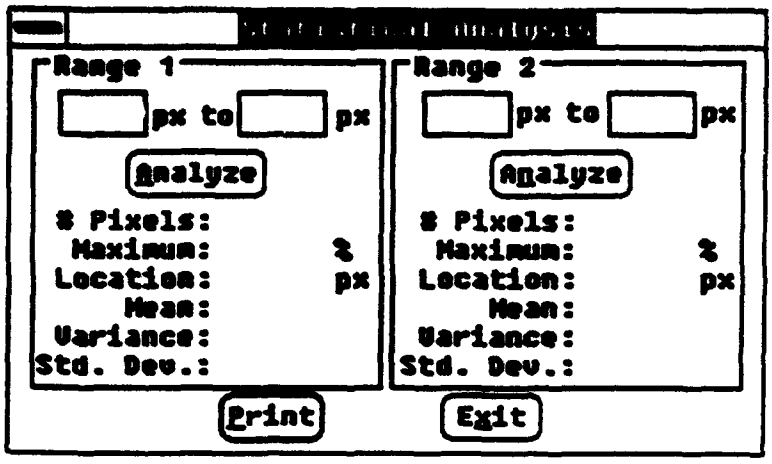


b)

October 26, 1992 STATISTICAL ANALYSIS 15:28:06

Range 1 1000 px to 1005 px

| | | |
|---|---|---|
| # Pixels | : | 6 |
| Maximum | : | 0.8 % |
| Location | : | 1003 px |
| Mean | : | 0.129 |
| Variance | : | 0.083 |
| Std. Dev. | : | 0.289 |

Range 2 1050 px to 1052 px

| | | |
|---|---|---|
| # Pixels | : | 3 |
| Maximum | : | 84.9 % |
| Location | : | 1051 px |
| Mean | : | 61.146 |
| Variance | : | 313.628 |
| Std. Dev. | : | 17.710 |

**Figure 12: Package for Statistical Analysis.**
**a) statistical analysis window,**
**b) statistical analysis results.**

a)

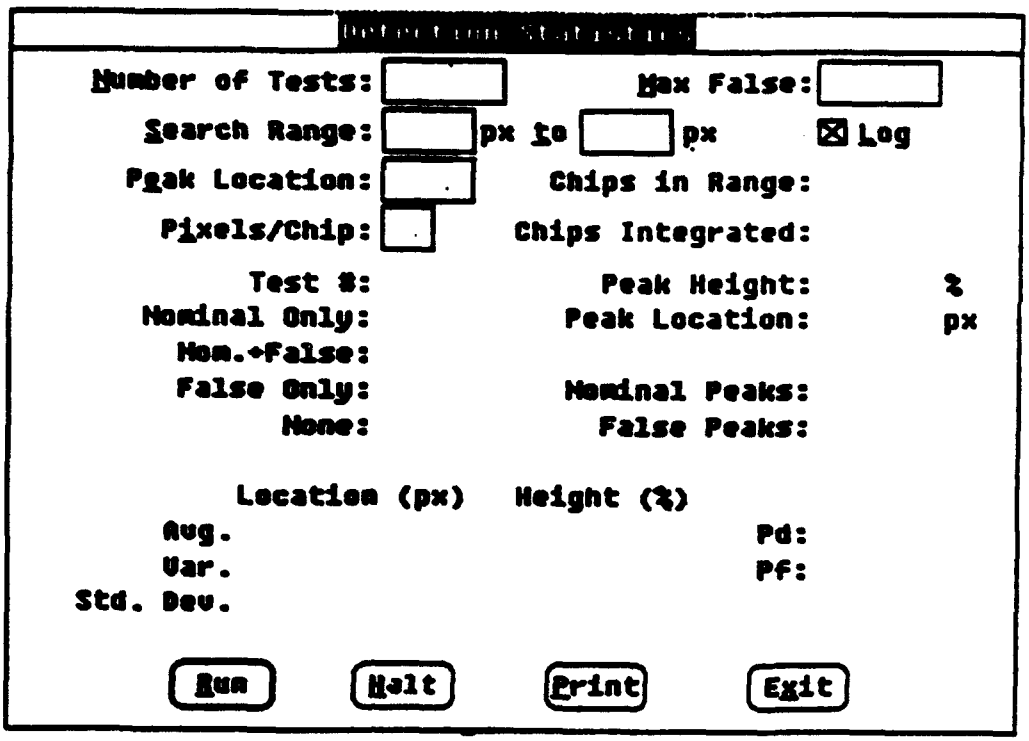


b)

October 26, 1992 DETECTION STATISTICS Page 1

Search Range: 4 px to 2043 px
Peak Location: 1051 px Chip Rate: MHz
Pixels/Chip: 5 px Integration Time: 3499 us
Chips in Range: 408 px Chips Integrated:

| | | |
|---|---|---|
| Tests: | 100 | |
| Nominal Only: | 100 | 100.0 % |
| Nom. + False: | 0 | 0.0 % |
| False Only: | 0 | 0.0 % |
| None: | 0 | 0.0 % |
| Nominal Peaks: | 100 | Pd: 1.000 |
| False Peaks: | 0 | Pf: 0.000 |

| | Peak Location (px) | Peak Height (%) |
|---|---|---|
| Average | 1050.8 | 87.1 |
| Variance | 0.3 | 1.0 |
| Std. Dev. | | 1.0 |

False Detection Log

| Test # | Pks | Loc. | Ht. | Loc. | Ht. | Loc. | Ht. |
|---|---|---|---|---|---|---|---|

Figure 13: Package for Detection Statistics.
a) detection statistics windows,
b) detection statistics results.

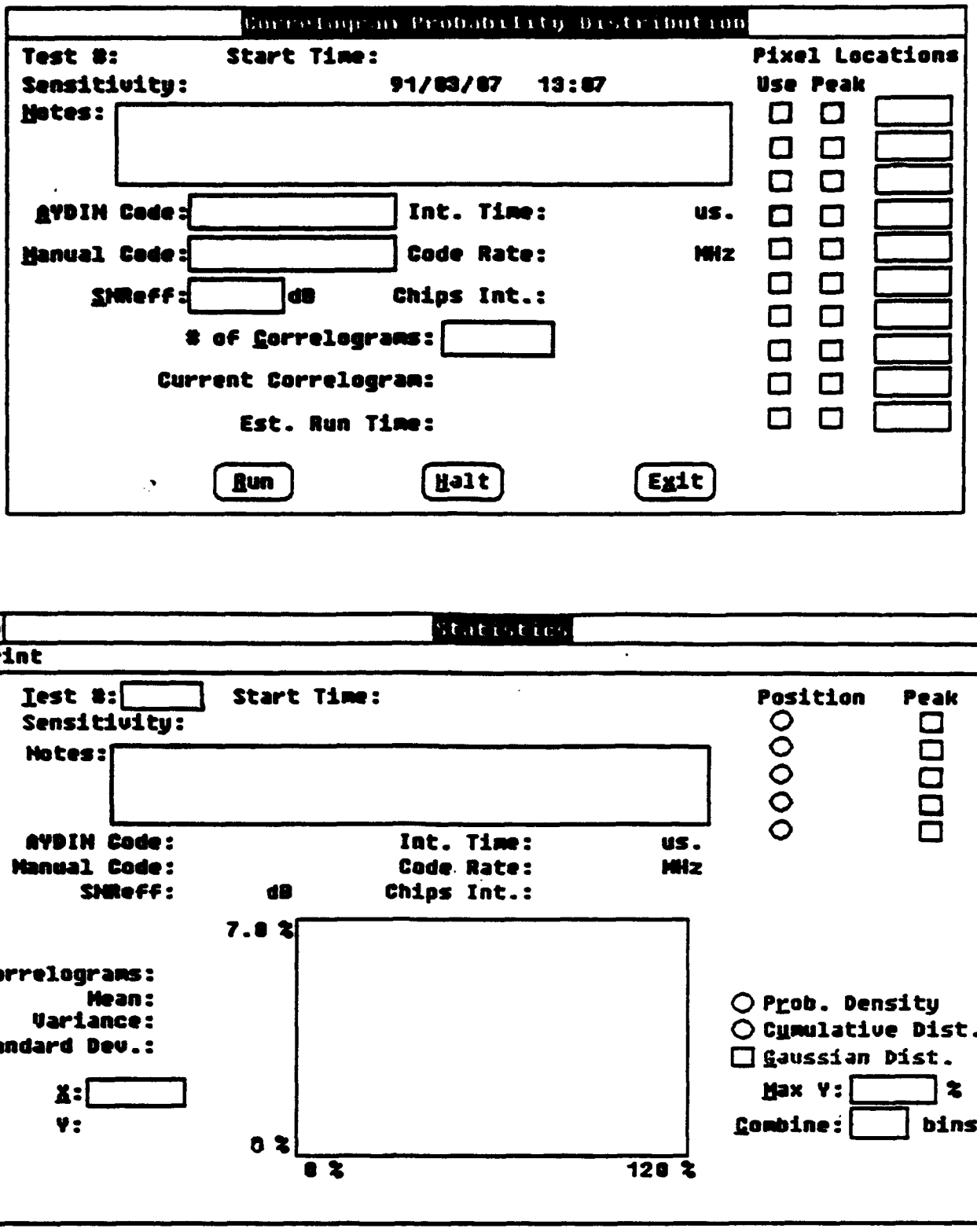


Figure 14: Example from the Probability Distribution Package:
a) probability distribution window,
b) results window.

October 27, 1992 PIXEL STATISTICS 07:07:18

Test Number: 50
Sensitivity File: CONSTANT.CSC
Correlograms: 1000

Started On: 92/10/26 15:41
Created On: 89/01/24 14:36

R8 AYDIN Code: 717
Manual Code: 717
Effective SNR: 100000.0 dB

Integration Time: 3499 us
Code Rate: 5 MHz
Chips Integrated: 17496.0

Position: 1051 (Peak)

Mean: 40.07
Variance: 0.46
Standard Dev: 0.68

Combined Bins: 1

Marker
X value: 0.05 %
Y Value: 0.000 %

Notes:

no noise

Probability Density

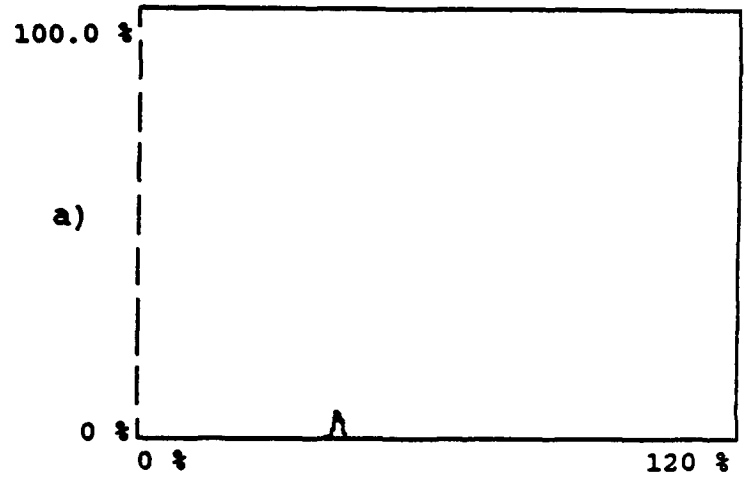


Cumulative Distribution

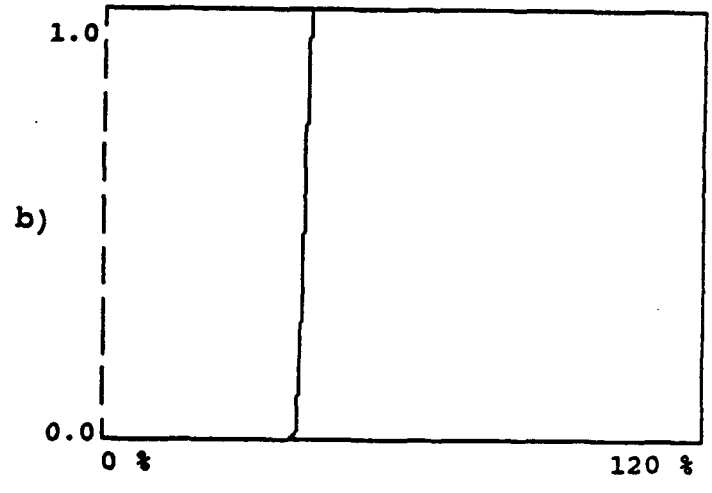


Figure 15: Example of Results from the Probability Distribution Package:
a) probability density,
b) cumulative distribution.

test. The tail probability is defined as the measured cumulative probability that the variable of the distribution function is larger than a certain number of standard deviations of the distribution. The probabilities of missing a peak P(md) and the of a false alarm P(fa) are also calculated and displayed.

## 5.0 CONCLUSION

A first version of a TIC has been designed and demonstrated at DREO. The great versatility of this prototype will allow many software algorithms to be tested and compared. Hardware implementations of these algorithms should substantially increase in the speed of more advanced versions.

The capability of the TIC to produce correlation has been demonstrated, and processing algorithms for statistical analysis have been developed. Three techniques of pedestal removal have been demonstrated.

However, the stability of the output still requires improvement. Fringes in the output could produce "blind spots" in the operating time-window. As a result, research will be undertaken to develop a strategy for data collection that is insensitive to the phase error that originates from the RF carrier or the optical system.

Work is planned on the design, construction, and testing of new, more compact architectures that would make the packaging of the system easier and facilitate the production of a stable output.

October 27, 1992 P(TAIL) STATISTICS 07:15:03

Test Number: 50 Started On: 92/10/26 15:41
Sensitivity File: CONSTANT.CSC Created On: 89/01/24 14:36
Correlograms: 1000

R8 AYDIN Code: 717 Integration Time: 3499 us
Manual Code: 717 Code Rate: 5 MHz
Effective SNR: 100000.0 dB Chips Integrated: 17496.0

| | PEAKS | 1051 |
|---|---|---|
| | Mean | 40.07 |
| | Standard Dev. | 0.68 |

| P(md) | Gaussian | |
|---|---|---|
| 0.159 | 1.00 | 1.12 |
| 0.1 | 1.28 | 1.41 |
| 0.05 | 1.64 | 1.78 |
| 0.025 | 1.96 | 2.03 |
| 0.01 | 2.33 | 2.42 |
| 0.001 | 3.09 | * |
| 0.0005 | 3.30 | * |
| 0.0002 | 3.55 | * |
| 0.0001 | 3.73 | * |
| 5E-005 | 3.90 | * |
| 2E-005 | 4.11 | * |
| 1E-005 | 4.27 | * |
| 5E-006 | 4.42 | * |

| | NOISE | 1000 | 1100 |
|---|---|---|---|
| | Standard Dev. | 0.05 | 0.05 |

| P(fa) | Gaussian | | |
|---|---|---|---|
| 0.318 | 1.00 | 0.68 | 0.68 |
| 0.2 | 1.28 | 0.80 | 0.80 |
| 0.1 | 1.64 | 0.90 | 0.90 |
| 0.05 | 1.96 | 0.95 | 0.95 |
| 0.02 | 2.33 | 0.98 | 0.98 |
| 0.002 | 3.09 | * | * |
| 0.001 | 3.30 | * | * |
| 0.0004 | 3.55 | * | * |
| 0.0002 | 3.73 | * | * |
| 0.0001 | 3.90 | * | * |
| 4E-005 | 4.11 | * | * |
| 2E-005 | 4.27 | * | * |
| 1E-005 | 4.42 | * | * |

Figure 16: Example of a Ptail Distribution from the Probability Distribution Package.

## 6.0 REFERENCES


[1] M.W. Casseday, N.J. Berg, I.J. Abramovitz and J.N. Lee, "Wide-band signal processing using the two-beam surface acoustic wave acoustooptic time integrating correlator", IEEE Transactions on Sonic and Ultrasonics, vol.SU-28, no.3, May 1981, p.205-212.

[2] N.J. Berg, M.W. Casseday, I.J. Abramovitz and J.N. Lee, "Radar and communication band signal processing using time-integrating processors", SPIE vol.232, 1980 International Optical Computing Conference, p.101-107.

[3] N.J. Berg, M.W. Casseday, A.N. Filipov and J.M. Pellegrino, "A new multifunction acousto-optic signal processor", 1983 Ultrasonics Symposium, p.454-458.

[4] B.V.K. Vijaya Kumar, D. Casasent and A. Goutzoulis,"Fine delay estimation with time integrating correlators", Appl. Optics, vol.21, no,21, 1 Nov. 1982, p. 3855-3863.

[5] I.J. Abramovitz, "Acousto-optic processors for passive surveillance", SPIE vol. 519, Analogue Optical Processing and Computing, 1984, p.2-8.

[6] I.J. Abramovitz, "Passive surveillance applications of acousto-optic processors", SPIE vol.545 Optical Technology for Microwave Applications II. 1985, p.102-107.

[7] N. Brousseau and R. Brousseau, "Analysis of DNA sequences by an optical time-integrating correlator: proposal", DREO TN 91-33.

[8] I.J. Abramovitz, N.J. Berg and M.W. Casseday, "Interferometric surface-wave acousto-optic time-integrating correlators", 1980 Ultrasonics Symposium, p.483-487.

[9] N.J. Berg, M.W. Casseday, I.J. Abramovitz and J.N. Lee, "Radar and communication band signal processing using time-integrating processors", SPIE vol.232, 1980 International Optical Computing Conference, p.101-107.

[10] C.S. Tsai, J.K. Wang and K.Y. Liao, "Acousto-optic time-integrating correlators using integrated optic technology", SPIE vol.180, Real-Time Signal Processing II, 1979, p. 160-163.

[11] M. Varasi, A. Vannucci and S. Reid, "Integrated acousto-optic correlator using the proton exchange technique",SPIE vol.1151, Optical Information Processing Systems and Architectures, 1989, p.457-466.

[12] N. J. Berg and J.N. Lee, "Acousto-optic signal processing: theory and implementation", Marcel Dekker Inc. New York and Basel, 1983, p.291.

[13] C.C. Lee, K.Y. Liao and C.S. Tsai, "Acoustooptic time-integrating correlator using hybrid integrated optics", 1982 IEEE Ultrasonics Symposium p. 405-407.

[14] W.T. Rhodes, "Acousto-optic signal processing: convolution and correlation", Proc. IEEE, vol.69, no.1, Jan. 1981, p.65-79.

[15] N. Laouar, J.P. Goedgebuer et R. Ferriere,"Corrélateur opto-électronique analogique pour le traitement en parallèle de signaux de type radar", Onzième colloque GRETSI- Nice 1-5 juin 1987, p.693-696.

[16] I.G. Fuss, "Acoustooptic signal processor based on a Mach-Zehnder interferometer", Appl.Opt. vol.24, no.22, 15 Nov 1985, p.3866-3871.

[17] D.A.B. Fogg, "A compact bulk acousto-optic time integrating correlator", Department of Defence of Australia, Technical Report ERL-0323-TR, Nov. 1984.

[18] M.S. Brown,"A Kosters prism time-integrating acousto-optic correlator", J. Phys, E:Sci. Instrum. 21 (1988) 192-194 p.192-194.

[19] N. Brousseau and J.W.A. Salt, "Design and implementation of a time-integrating correlator using a bulk acousto-optics interaction",Defence Research Establishment Ottawa technical Note 86-25, Sept. 1986.

[20] R.A. Sprague and C.L. Kolicpoulos, "Time integrating acoustooptic correlator", Appl.Opt. vol.15, no.1, Jan 1976, p.89-92.

[21] G. Silbershatz and D. Casasent, "Hybrid time and space integrating processors for spread spectrum applications", Appl. Opt., vol.22, no.14, 15 July 1983, p.2095-2103.

[22] D. Casasent, "General time-, space-, and frequency-multiplexed acoustooptic correlator", Appl. Optics, vol.24, no.17, 1 Sept. 1985., p. 2884-2888.

[23] F.B. Rotz, "Time-integrating optical correlator", SPIE vol. 202, Active Optical Devices, 1979, p.163-169.

[24] P. Kellman, "Time-integrating optical signal processing", Stanford University, Dept. of Electrical Engineering, Ph.D. dissertation, June 1979.

[25] D. Casasent, A. Goutzoulis and V.K. Vijaya Kumar, "Time-integrating acoustooptic correlator: error source modelling", Appl. Opt., vol.23, no.18, 15 Sept. 1984, p.3130-3137.

[26] S. Wofford, G. Petrie and D.L. Hecht," Polarization effects in shear wave tellurium dioxide acousto-optic devices", SPIE vol. 202 Active Optical Devices, 1979, p. 180- 185.

[27] M. Amano, G. Elston and J. Lucero, "Materials for large time aperture Bragg cell", SPIE vol.567, Advances in Materials for Active Optics, 1985, p.142-149.

[28] G. Elston, "Optically and Acoustically Roteated Slow Shear Bragg Cells in $TeO_2$", SPIE vol.936, Advances in Optical Information Processing, 1988, p.95-101.

[29] E.H. Young and H.C. Ho, "Optically Rotated Long Time Aperture TeO2 Bragg cell", SPIE vol. 1296 Advances in Optical Information Processing IV, 1990, p.304-315.

[30] J.N. Lee, N.J. Berg, M.W. Casseday and P.S. Brody, "High-speed adaptive filtering and reconstruction of broadband signals using acousto-optic techniques", IEEE Ultrasonics Symposium Proceedings, 1980, p.488.

[31] S.D. Fantane, "Anamorphic Prism: A New Type", Applied Optics, Vol. 30, no. 34, 1 Dec 1991, p. 5008-5009.

[32] A.H. Firester, T.E. Gayeski and M.E. Heller, "Efficient Generation of Laser Beams with an Elliptic Cross Section", Applied Optics, Vol. 11, No. 7, July 1972, p 1648-1649.

[33] W. Veldkamp and E.Van Allen, "Compact, Collinear, and Variable Anamorphic-Beam Compressor Design", Applied Optics, Vol. 21, No. 1, 1 Jan. 1982, p 7-9.

[34] D. Malacara, "Optical shop testing", John Wiley and Sons, 1978.

[35] C. Bélisle, N. Brousseau and J.W.A Salt, "Evaluation procedure for linear array photosensitive detectors: applications to CSF TH 7805", DREO TN 89-6.

[36] "Acousto-Optical Signal Processing Development Facility: Time-Integrating Correlator/Operator Manual", Miller Communications Systems Ltd., DSS contract number W7714-7-5396.

[37] "Acousto-Optical Post-Processor Development Facility: Time-Integrating Correlator/Software Manual", Miller Communications Systems Ltd., DSS contract number W7714-7-5396.

[38] "Acousto-Optical Signal Processing Development Facility: Time-Integrating Correlator/Detailed Design Information", Miller Communications Systems Ltd., DSS contract number W7714-7-5396.

[39] "Acousto-Optical Signal Processing Development Facility: Time-Integrating Correlator/Hardware Manual", Miller Communications Systems Ltd., DSS contract number W7714-7-5396.

[40] S.W. Golomb, "Shift Register Sequences", Holden-Day, San Francisco, 1967.

[41] R.C. Dixon, "Spread Spectrum Systems", John Wiley & Sons, New York, Second Edition, 1984, p. 77.

[42] "Acousto-Optical Post-Processor/Time-Integrating Correlator Updates: Final Report", Calian Communications Systems Ltd., DSS Contract Number W7714-0-9886.

[43] "Acousto-Optical Post-Processor/Time-Integrating Correlator: Updates", Calian Communications Systems Ltd., DSS Contract Number W7714-1-9981, 9982.

## DOCUMENT CONTROL DATA

(Security classification of title, body of abstract and indexing annotation must be entered when the overall document is classified)

1. ORIGINATOR (the name and address of the organization preparing the document. Organizations for whom the document was prepared, e.g. Establishment sponsoring a contractor's report, or tasking agency, are entered in section 8.)

DEFENCE RESEARCH ESTABLISHMENT OTTAWA
NATIONAL DEFENCE
SHIRLEY BAY, OTTAWA, ONTARIO K1A 0K2 CANADA

2. SECURITY CLASSIFICATION (overall security classification of the document. including special warning terms if applicable)

UNCLASSIFIED

3. TITLE (the complete document title as indicated on the title page. Its classification should be indicated by the appropriate abbreviation (S,C or U) in parentheses after the title.)

DESIGN AND DEMONSTRATION OF AN ACOUSTO-OPTIC TIME-INTEGRATING CORRELATOR WITH A LARGE PARALLEL GAIN (U)

4. AUTHORS (Last name, first name, middle initial)

BROUSSEAU, N., AND SALT, J.W.A.

5. DATE OF PUBLICATION (month and year of publication of document)

JANUARY 1993

6a. NO. OF PAGES (total containing information. Include Annexes, Appendices, etc.)

31

6b. NO. OF REFS (total cited in document)

38

7. DESCRIPTIVE NOTES (the category of the document, e.g. technical report, technical note or memorandum. If appropriate, enter the type of report, e.g. interim, progress, summary, annual or final. Give the inclusive dates when a specific reporting period is covered.)

DREO TECHNICAL NOTE

8. SPONSORING ACTIVITY (the name of the department project office or laboratory sponsoring the research and development. Include the address.)

DEFENCE RESEARCH ESTABLISHMENT OTTAWA
NATIONAL DEFENCE
SHIRLEY BAY, OTTAWA, ONTARIO K1A 0K2 CANADA

9a. PROJECT OR GRANT NO. (if appropriate, the applicable research and development project or grant number under which the document was written. Please specify whether project or grant)

041LQ

9b. CONTRACT NO. (if appropriate, the applicable number under which the document was written)

10a. ORIGINATOR'S DOCUMENT NUMBER (the official document number by which the document is identified by the originating activity. This number must be unique to this document.)

DREO TECHNICAL NOTE 93-24

10b. OTHER DOCUMENT NOS. (Any other numbers which may be assigned this document either by the originator or by the sponsor)

11. DOCUMENT AVAILABILITY (any limitations on further dissemination of the document, other than those imposed by security classification)

- ( X ) Unlimited distribution
- ( ) Distribution limited to defence departments and defence contractors; further distribution only as approved
- ( ) Distribution limited to defence departments and Canadian defence contractors; further distribution only as approved
- ( ) Distribution limited to government departments and agencies; further distribution only as approved
- ( ) Distribution limited to defence departments; further distribution only as approved
- ( ) Other (please specify):

12. DOCUMENT ANNOUNCEMENT (any limitation to the bibliographic announcement of this document. This will normally correspond to the Document Availability (11). However, where further distribution (beyond the audience specified in 11) is possible, a wider announcement audience may be selected.)

UNCLASSIFIED

SECURITY CLASSIFICATION OF FORM

13. ABSTRACT ( a brief and factual summary of the document. It may also appear elsewhere in the body of the document itself. It is highly desirable that the abstract of classified documents be unclassified. Each paragraph of the abstract shall begin with an indication of the security classification of the information in the paragraph (unless the document itself is unclassified) represented as (S), (C), or (U). It is not necessary to include here abstracts in both offical languages unless the text is bilingual).

(U) Time-Integrating Correlators (TICs) have been implemented using either surface (integrated optics) or bulk acousto-optic interaction. The purpose of this technical note is to document the development of a signal processing facility that includes a TIC designed to operate with a large parallel gain and a Digital Post-Processor (DPP). The DPP controls the input signals to the TIC and the collection and analysis of the optical data produced by the TIC. A brief review of the principle of operation of TICs is presented together with discussions about the selection criteria for the various components and the compromises involved. A description of the DPP facility and of the algorithms available to analyse the output of the TIC is also included.

14. KEYWORDS, DESCRIPTORS or IDENTIFIERS (technically meaningful terms or short phrases that characterize a document and could be helpful in cataloguing the document. They should be selected so that no security classification is required. Identifiers, such as equipment model designation, trade name, military project code name, geographic location may also be included. If possible keywords should be selected from a published thesaurus, e.g. Thesaurus of Engineering and Scientific Terms (TEST) and that thesaurus-identified. If it is not possible to select indexing terms which are Unclassified, the classification of each should be indicated as with the title.)

TIME-INTEGRATING CORRELATOR
OPTICAL DATA PROCESSING
OPTICAL CORRELATOR